NRAGE Mediates p38 Activation and Neural Progenitor Apoptosis via the Bone Morphogenetic Protein Signaling Cascade

Stephen E. Kendall,[1]* Chiara Battelli,[2,3] Sarah Irwin,[4] Jane G. Mitchell,[3]
Carlotta A. Glackin,[1] and Joseph M. Verdi[3]

City of Hope/Beckman Research Institute, Department of Molecular Medicine, Duarte, California[1]; Department of Medical Oncology, Catholic University, Rome, Italy[2]; University of Western Ontario, London, Ontario, Canada[4]; and Maine Medical Center Research Institute, Center for Regenerative Medicine, Portland, Maine[3]

Understanding the molecular events that govern neural progenitor lineage commitment, mitotic arrest, and differentiation into functional progeny are germane to our understanding of neocortical development. Members of the family of bone morphogenetic proteins (BMPs) play pivotal roles in regulating neural differentiation and apoptosis during neurogenesis through combined actions involving Smad and TAK1 activation. We demonstrate that BMP signaling is required for the induction of apoptosis of neural progenitors and that NRAGE is a mandatory component of the signaling cascade. NRAGE possesses the ability to bind and function with the TAK1-TAB1-XIAP complex facilitating the activation of p38. Disruption of NRAGE or any other member of the noncanonical signaling cascaded is sufficient to block p38 activation and thus the proapoptotic signals generated through BMP exposure. The function of NRAGE is independent of Smad signaling, but the introduction of a dominant-negative Smad5 also rescues neural progenitor apoptosis, suggesting that both canonical and noncanonical pathways can converge and regulate BMP-mediated apoptosis. Collectively, these results establish NRAGE as an integral component in BMP signaling and clarify its role during neural progenitor development.

The pseudostratified neuroepithelium of the neural tube is generated from neural progenitor cells located within the ventricular and subventricular zones. The fate of neural progenitors is defined by their microenvironment, including effects from tissue outside the central nervous system (31, 35, 36). The generation of specific cellular phenotypes, neurons, astrocytes, radial glia, and oligodendrocytes occurs during tightly regulated spatial and temporal windows throughout embryogenesis and early postnatal life. Regulation is complex, requiring transitional changes in intrinsic cues and the availability of extrinsic growth, differentiation and survival factors. Adding to this complexity is the recognition that programmed cell death or apoptosis is a prominent event that regulates cell numbers throughout the entire pathway from neural progenitor to mature differentiated phenotype (1, 2, 6, 34). The regulation of cell numbers during each stage of neural development may be important for the correct temporal and spatial generation of cell phenotypes and consequently normal brain morphogenesis.

The fate of neural progenitor cells (NPCs) is regulated in part by bone morphogenetic proteins (BMPs), which are members of the transforming growth factor β superfamily (TGF-β). BMPs signal through binding a heterotetrameric complex of type I (BMPR-I) and type II (BMPR-II) serine-threonine kinase receptors (45). The "canonical" pathway activates Smad1, Smad5, and Smad4 proteins (13). However, an alternative signaling pathway was recently described in which the X-linked inhibitor of apoptosis protein (XIAP) functions as an adaptor protein bridging BMPR-Ia and TGF-β activated binding protein (TAB1), an activator of the MAPKKK TGF-β activated kinase 1 (TAK1) (41, 49, 50). TAK1 activity promotes activation of p38 (18, 29), Jun N-terminal kinases (JNKs) (42, 51), and Nemo-like kinase (14), which is a mitogen-activated protein kinase (MAPK) family member.

The multiple functions of BMPs during embryogenesis and neural development include complex actions upon the neural crest (11, 43), apoptosis or differentiation of neurons and glia within the cortex (3, 21, 23, 33) and dorsal spinal cord (16). These apoptotic actions may be initiated through TAK1, which induces apoptosis in the neuroepithelium of *Xenopus* embryos (40). Another prominent regulator of cell death is XIAP, which can directly bind to and inhibit the activity of caspases. More recently, XIAP has been shown to bind TAB1 to activate TAK1 and inhibit TAK1-induced apoptosis (49).

Collectively, these observations argue that BMPs regulate key events during neurogenesis. The mechanism that governs a seemingly paradoxical switch between morphogenesis and apoptosis within the developing cortex remains unclear. However, recent work suggests that at embryonic day 13 (E13), the onset of corticogenesis in the mouse, high levels of BMPs (10 to 100 ng/ml) promote apoptosis and inhibit proliferation of neural progenitor cells of the ventricular zone (6, 21, 23). Moreover, by the midpoint of neurogenesis (E16), BMPs promote neural differentiation of neural progenitors (23, 33). It appears that neural and glial progenitors secrete BMPs directing both neurogenesis and gliogenesis in a concentration-dependent manner to make the critical switch to neurotrophin signals and related cytokines (3, 52).

Neurotrophin receptor interacting MAGE (NRAGE) homologue was originally characterized through a screen for pro-

* Corresponding author. Mailing address: City of Hope/Beckman Research Institute, 1500 E. Duarte Rd., Duarte, CA 91010. Phone: (626) 301-8896. Fax: (626) 301-8121. E-mail: skendall@coh.org.

TABLE 1. Morpholino sequences and knockdown efficiency

Morpholino	Sequence	P19 cell delivery efficiency	P19 cell knockdown efficiency (%)	NP cell delivery efficiency (%)	NP cell knockdown efficiency (%)
NRAGE	5'-GGTTTCTGAGCCATAGCTCTCGTC-3'	90	80	60	78
TAK1	5'-AGCGCCCTTCAGCCCGGAGCCC-3'	92	85	65	78
p53	5'-GACTCCATGGCAGTCATCCAGT-3'	94	83	62	83
Standard control	5'-CCTCTTACCTCAGTTACAATTTATA-3'	90	0	59	0

teins that interact with the intracellular domain of the p75 neurotrophin receptor (p75^{NTR}). NRAGE was shown to mediate both cell cycle withdrawal and a nerve growth factor-specific apoptosis in sympathetic precursor cells through p75^{NTR} (38). NRAGE is expressed during early corticogenesis, specifically in neural progenitors of the ventricular zone and in differentiating neuroblasts of the cortex, independent of p75^{NTR} expression and concomitant with the spatial and temporal occurrence of BMP-mediated apoptosis (17). This p75^{NTR}-independent expression suggests an alternative signaling cascade that may utilize NRAGE to regulate mitotic arrest and apoptosis of neural progenitors. In support of this p75^{NTR}-independent function, NRAGE was shown to augment interleukin-3-withdrawal-induced apoptosis through binding endogenous XIAP (15), and NRAGE is involved in UNC5-H1 induced apoptosis of sympathetic neural progenitors (48). Additional studies suggest that NRAGE associates with the BMP-regulated homeobox transcription factors Msx2 and Dlx5 and translocates to the nucleus (26, 39). Collectively, these results suggest that NRAGE may function in the BMP signaling cascade to regulate early neural progenitor apoptosis.

Based on the temporal and spatial appearance of NRAGE in the ventricular zone, an active area of cell cycle withdrawal and BMP-induced apoptosis, we investigated whether NRAGE was involved in these events during cortical neurogenesis. Using a loss-of- and gain-of-function approach, NRAGE expression was shown to be a prerequisite to mediate apoptosis of NPCs through a BMPR-Ia-dependent pathway. Activation of BMPRs leads to the formation of the TAK1-TAB1-XIAP signaling complex in which NRAGE is a crucial component regulating p38 activity. Under BMPR stimulation, NRAGE facilitates the formation of a TAK1-TAB1-XIAP-NRAGE complex that activates p38, driving cellular apoptosis in neural progenitor cells. The ability for NRAGE to regulate this MAPK signaling is fundamentally important for neural progenitor survival, positioning NRAGE as a key molecule during neocortical development independent of its role in neurotrophin signaling events.

MATERIALS AND METHODS

Cell culture. P19 embryonal carcinoma cells were maintained in growth medium consisting of α-MEM (Invitrogen), 7.5% heat-inactivated calf serum, and 2.5% heat-inactivated fetal calf serum (HyClone) at 37°C in 5% CO_2. For apoptosis assays, cells were seeded at a concentration of 10^5 cells/ml in bacteriological-grade culture dishes in growth media supplemented with 1 μM all-trans-retinoic acid (RA) and/or 10 ng of recombinant BMP-4 (R&D Systems)/ml or without supplementation for 1 to 4 days. For neural differentiation, P19 cells were grown as aggregates in the presence of 1 μM RA for 4 days, treated with trypsin, and transferred to fibronectin-coated tissue culture dished in the absence of RA for an additional 4 days. Cortical neural progenitors were isolated from E13 embryos through aseptic removal and placed in Hanks balanced salt solution (Invitrogen) supplemented with 10% fetal bovine serum. Cerebral cortex was

removed from each, freed of meninges, dispersed with 0.05% trypsin-EDTA, and filtered with 70-μm-pore-size nylon cell strainers (VWR). Cells were seeded (2 × 10^5 cells/ml) as aggregates in a medium containing 38% neurobasal medium, 60% Dulbecco modified Eagle medium-F12, 2% fetal bovine serum, N2 supplemented (Invitrogen), and 0.4 μl of penicillin-streptomycin (Invitrogen)/ml.

Overexpression and loss-of-function studies. Overexpression studies were performed by using mammalian expression vectors containing NRAGE-EGFP, NRAGE-myc, and an empty vector-EGFP, wild-type and dominant-negative BMPR-Ia, and a dominant-negative Smad5. Cells were transfected via Lipofectamine 2000 according to the manufacturer's recommended protocol (Invitrogen). Loss-of-function studies used the use of antisense morpholinos directed to the start sites of the genes of interest (see Table 1 for sequences and delivery and knockdown efficiencies) and delivered by using EPEI as recommended by the manufacturer (Gene Tools).

Morpholinos incorporated a fluorescein tag to identify cells that have taken up the morpholino sequence, allowing purification of the population if required by fluorescence-activated cell sorting (FACS). The specific p38 MAPK antagonist SB203580 was used at a concentration of 5 μM (Calbiochem).

Immunoblotting and immunoprecipitation. The following antibodies were used for biochemical analysis: α-caspase-3 (Pharmingen), α-TAK1, α-p38, α-dp-p38, α-JNK1/2, α-β-actin (Sigma), α-XIAP, α-BMPR-Ia, α-BMPR-1b, α-SMAD1, α-SMAD5, α-TAB1, α-GFP (Santa Cruz), α-NFκBp65 (BD Biosciences), α-NRAGE$_{53-295}$, α-N-myc, α-pSMAD1, α-pRB, α-p-pRB, α-p53, α-p21^{waf1}, and α-p27^{kip1} (Upstate). For biochemical analysis, whole-cell extracts were prepared by using Nonidet P-40 (NP-40) lysis buffer (137 mM NaCl, 20 mM Tris [pH 8.0], 0.5 mM EDTA, 10% glycerol, 1% NP-40) containing a protease inhibitor cocktail (Roche) supplemented with 1 mM sodium orthovanadate and 1.25 mM sodium fluoride. The concentration of total soluble protein was measured by using a BCA protein assay kit (Pierce). Lysates were immunoprecipitated by using 50 μg of protein, 0.1 μl (vol/vol) pansorbin (Calbiochem), 1 μg of α-N-Myc/ml, or α-GFP antibody overnight at 4°C. Immunoprecipitations were washed three times with lysis buffer and subjected to sodium dodecyl sulfate-polyacrylamide gel electrophoresis immunoblotting. For both immunoblotting and immunoprecipitation experiments, 50 μg of cell lysate was subjected to sodium dodecyl sulfate-polyacrylamide gel electrophoresis using a 7 to 15% polyacrylamide gel under reducing conditions. After semidry transfer onto Immobilon-P (Millipore), membranes were probed with appropriate primary antibody. Primary antibody detection was accomplished by using an appropriate secondary horseradish peroxidase conjugate immunoglobulin Gs (Jackson Immunoresearch, Inc.), developed with a chemiluminescent reagent (Amersham), and exposed to Kodak Film for 1 and 2 min.

Apoptosis and cell survival assays. The number of viable and nonviable cells was determined by trypan blue exclusion. An equal volume of 0.4% trypan blue solution (Sigma) was added to the medium and left for 1 min. The numbers of total and stained cells were counted within 5 min with a hemocytometer. All apoptosis and FACS analyses were performed with a Becton Dickinson FACS-Vantage SE cell sorter. Live cells were collected at 24 and 48 h after apoptotic induction and labeled with annexin V biotin that was subsequently detected by using streptavidin-phycoerythrin secondary antibodies. For annexin V assays, 10 μg of 7-actinomycin D/ml was used as a cell-impermeable vital dye for discriminating early (annexin V$^+$/7-AAD$^-$) and late apoptosis or necrotic cell death (annexin V$^+$/7-AAD$^+$). Additional measures of apoptosis used the characterization of mitochondrial membrane permeability as determined by the MitoCapture assay kit (Calbiochem) and analyzed by flow cytometry according to manufacturer's specifications.

Cell cycle analysis. For cell cycle analysis, P19 cells overexpressing the genes of interest were synchronized in G$_0$/G$_1$ by using standard serum withdrawal. Briefly, cells were cultured in serum-free conditions for 6 h and transfected in serum-free conditions for an additional 6 h. Upon conclusion, serum-containing medium was replaced, and cells were permitted to grow for an additional 24, 48, or 72 h. Live cells were collected, stained by using a hypotonic DNA staining

TABLE 2. RT-PCR primer sequences

Gene	Forward primer (5'-3')	Reverse primer (3'-5')	Annealing temp (°C)
Oct3/4	ATGGCTGGACACCTGGCTTCAGACT	GCCAGGCTCCTGATCAACAGCATCA	63
Hes1	AGAAGAGGCGAAGGGCAAGAA	CAAAAAACCTTGGCAGCCTCT	54
Mash1	TCGGCACTGACTTTTGCGGCTGCTTT	GAAGCACGATCAAAGGGGGACGAA	56
Wnt-1	ACGTTGCTACTGGCACTGAC	CCATTTGCACTATCGCACAG	58
Neuro D1	TCAGCATCAATGGCAACT	TGACTCGCTCATGATGCGA	56
MEF2A	AGAAATGCCGACAGCCTACAA	TCACCCATGTGTCCATCCTCA	54
MEF2C	AGCAAGAATACGATGCCATC	GAAGGGGTGGTGGTACGGTC	56
Dlx5	CCGTCTCAGGAATCGCCAAC	CTGAAAGCTGGCTGGCTGGT	56
Msx2	ATTCGCCGCCGCCAAGACATA	TCTTTTCGCCTTGGCCCTTCG	56
β-Actin	TGTTACCAACTGGGACGACA	CTCTCAGCTGTGGTGGTGAA	56

solution (1 mg of sodium citrate/ml, 0.3% Triton X-100, 0.1 mg of propidium iodide/ml, 20 μM RNase A/ml), and DNA content was analyzed on a Becton Dickinson FACSCalibur by using Modfit 2.0 software. NRAGE^{+GFP} or control^{+GFP} cells were gated and DNA content was measured on FL2-area. The baseline location of the $G_0/G1$ peak was set for the control^{+GFP} cells and determined independently for each replicate.

Immunocytochemistry. Adherent cultures were grown on fibronectin-coated glass coverslips. After 4 days cells were fixed in 4% paraformaldehyde in phosphate-buffered saline for 10 min, rinsed in phosphate-buffered saline, and labeled with the postmitotic neural markers MAP2a/b, the astrocyte specific marker glial fibrillary acidic protein (GFAP) (Sigma), and Nestin, which labels multipotential progenitors (Pharmingen). Appropriate species-specific secondary antibodies conjugated to rhodamine were used together with the DNA-binding dye Hoechst 33258 (1 μg/ml). The percentage of cell phenotypes was obtained for each replicate as the average of four frames.

Semiquantitative reverse transcription-PCR (RT-PCR). Total RNA was isolated, treated with 1 U of DNase I at room temperature, and reprecipitated. First-strand cDNA was synthesized from 5 μg of total RNA with Superscript II (Invitrogen) by using an Oligo(dT)$_{12-18}$ (Invitrogen) primer according to published procedures (17). All PCRs were performed in the linear range of amplification as determined empirically by using 1 μl for each cDNA sample generated. Whenever possible, primers were designed to cross an intron-exon border to distinguish cDNA amplification from any potential genomic contamination. Primer sequences and annealing temperatures are given in Table 2.

The cycling parameters were as follows: denaturing at 94°C for 30 s, annealing temperature (primer specific, see Table 2) for 30 s, and extension at 72°C for 1 min. Amplification products were separated on a 1% agarose gel and visualized with ethidium bromide.

Statistics. All data are presented as the means ± the standard deviations (SD) of at least four independent experiments. Significance was determined by using the Student t test.

RESULTS

NRAGE is required in the BMP-mediated RA-induced apoptosis. Because NRAGE was expressed within the developing central nervous system in the absence of p75^{NTR} (17), we sought to determine whether NRAGE played a key role in the formation of the nervous system outside the roles mediated by neurotrophins. To this end, we utilized two prominent cell culture models: P19 embryonal carcinoma cells and cortical neural progenitors (NPCs) isolated from E13 embryos. RT-PCR analysis demonstrated that P19 cells which were treated with RA to stimulate apoptosis failed to express p75^{NTR} receptor (Fig. 1A) and neural progenitors began to express p75^{NTR} only after differentiation in culture (Fig. 1A).

Retinoic acid (RA) has previously been shown to induce apoptosis of P19 cells through the BMP signaling pathway. Using two independent measures of cell survival, trypan blue exclusion and annexin V immunoreactivity, we found that P19 cell viability was greatly compromised when treated with a combination of RA and BMP-4 than when treated with either of these alone (Fig. 1B to D). We attempted exacerbate the effects of RA on developing neuroblasts by overexpressing BMPR-Ia and treating the resulting cells with RA. Cell survival decreased precipitously (52% ± 2%) to a level comparable to that of the cells treated with RA and BMP-4 (48% ± 1%). In contrast, in cells in which BMP signaling was diminished by the expression of a dominant-negative allele of BMPR-Ia, which expresses only the extracellular domain, cell viability in the presence of RA was enhanced and approached the level of untreated controls (RA treated, 72% ± 2%; RA + dnBMPR-Ia, 85% ± 1% [$P \leq 0.01$]; untreated, 95% ± 1%). Moreover, RT-PCR analysis demonstrated that BMP-2 and BMP-4 transcripts were greatly elevated after RA exposure (data not shown). These results support the hypothesis that RA-induced apoptosis of proliferating neuroblasts is mediated by BMP signaling pathways.

We then sought to determine whether NRAGE had any role in mediating cell survival in either cell system treated with RA and BMP-4. Cell viability was greatly enhanced in RA- and BMP-4-treated cells that underexpressed NRAGE using specific antisense morpholinos (Fig. 1E and F). Conversely, the vast majority of P19 cells overexpressing NRAGE underwent cell death within 48 h, even in the absence of RA and BMP-4 treatment (Fig. 1D). The addition of RA and BMP-4 only enhanced the effect and the time course of apoptosis in NRAGE overexpressing cells. These data, taken together, demonstrate that the cell death signal initiated by RA and BMP-4 is relayed by the BMP signal transduction cascade and requires NRAGE.

To further confirm the link between NRAGE and RA- and BMP-4-mediated apoptosis, we examined the expression of NRAGE protein as a function of time after RA and BMP-4 treatment. NRAGE protein levels rose sharply in P19 cells 1 day after induction with RA and/or BMP-4 (Fig. 2A) and in primary NPCs (Fig. 2B). The elicited levels of NRAGE correlated with an increase in active caspase-3 in both systems. The activation of caspase-3 was abrogated in cells where NRAGE levels were reduced (Fig. 2A and B), and activation was conversely enhanced in NRAGE-overexpressing cells. These results suggest that NRAGE plays a pivotal role in mediating RA and/or BMP-4 induction of caspase-3, leading to apoptosis.

NRAGE interacts with members of the BMP signaling cascade to promote p38 activation. NRAGE's role in RA- and BMP-4-induced apoptosis prompted clarification of whether
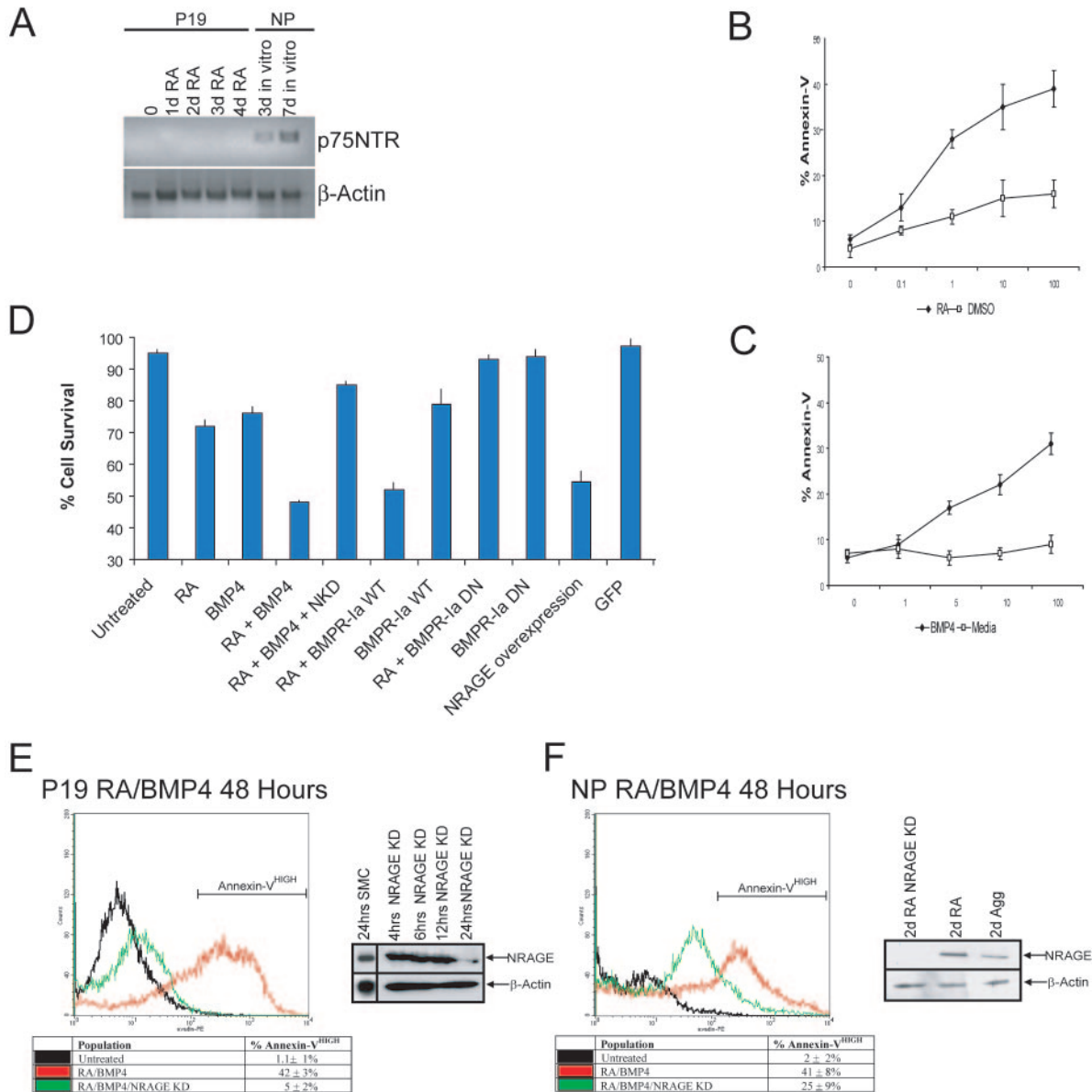
FIG. 1. RA-induced apoptosis is mediated through BMP signaling. (A) RNA was isolated from P19 cells treated with RA over a 4-day period and from E13 neural progenitors after 3 or 7 days of in vitro differentiation. P19 cells do not express p75[NTR], but postmitotic neurons cultured from NPCs are p75[NTR] positive. (B and C) Dose-response curves were generated to determine effective dosages of either RA or BMP-4 for the induction of apoptosis in P19 cells. (D) P19 cell survival was measured by using trypan blue exclusion after apoptotic induction with 10 ng of BMP-4/ml, 1 μM RA, or both. Means ± the SD of four independent experiments demonstrate that RA enhances the number of dyeing cells utilizing the BMP signaling pathway. (E and F) Representative FACS histograms of P19 and NPCs treated with 10 ng of BMP-4/ml and 1 μM RA. Western analysis demonstrated the extent of NRAGE suppression using NRAGE antisense morpholinos relative to standard morpholino control. Note that the suppression of NRAGE expression (NRAGE KD) in both cortical progenitors and P19 cells limits the percentage of annexin V, apoptotic cells.

NRAGE functions directly or indirectly in the BMP signaling cascade. To this end, we performed immunoprecipitation experiments with myc-tagged NRAGE overexpressed in P19 cells treated with BMP-4. Cell lysates were collected, and Western analyses were performed with antibodies specific to endogenous members of the BMP signaling cascade. Tagged NRAGE was found to weakly associate with the BMP receptors BMPR-II and BMPR-Ia, whereas it showed a strong association with BMPR-Ib. Since both BMPR-I and BMPR-II are capable of existing as a heterotetramer when activated, immu-

noprecipitation of both type I and type II receptors with NRAGE was not unexpected (Fig. 3A).

The most understood mode of BMP signaling within the cell utilizes members of the Smad family. Both Smad1 and Smad5 were found to only weakly associate with the NRAGE complex. Interestingly, NRAGE was found to strongly interact with TAK1, TAB1 and XIAP (Fig. 3A). These proteins are all members of a lesser-known pathway downstream of the BMP receptor, which has been shown to promote the activation of p38. We surmised that NRAGE interaction with these mem-
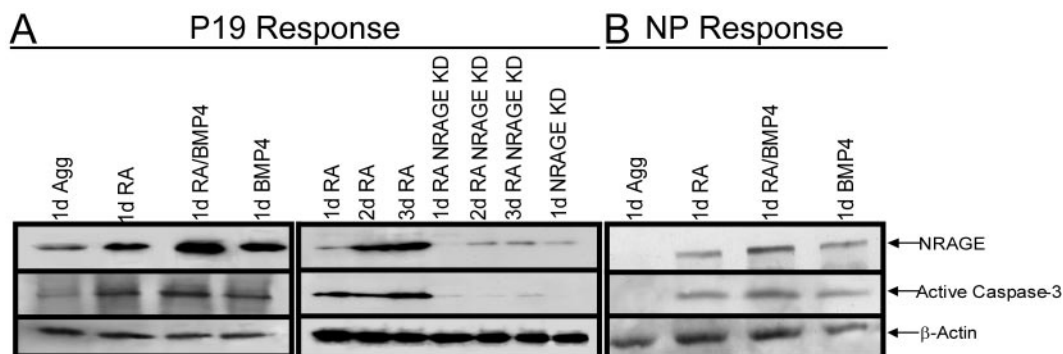
FIG. 2. NRAGE is required for the activation of caspase-3 by RA and BMP-4. Lysate of P19 or NPCs harboring control morpholinos or NRAGE morpholinos treated with RA, BMP-4, or both were collected daily and subjected to Western analyses to determine the levels of NRAGE and active caspase-3 during apoptosis. In the absence of NRAGE expression, caspase-3 was not active, and this correlated with enhanced cell survival.

bers of the BMP signaling pathway is specific since there was no association between NRAGE and BMP-independent TAK1-binding proteins NF-kβp65 and Bcl-2 (Fig. 3A and data not shown), suggesting that the main mode of BMP apoptotic activity is through this noncanonical signaling pathway of TAK1, TAB1, and XIAP.

Following our initial observation that when NRAGE was overexpressed, application of BMP-4 significantly enhanced the capacity for NRAGE to associate with members of the BMP signaling cascade (Fig. 3A). However, in the absence of ligand stimulation, prolonged NRAGE overexpression resulted in cellular apoptosis, suggesting that accumulation of NRAGE can force activation of the BMPR complex involving both canonical and noncanonical signaling. However, in the absence of BMP-4 NRAGE overexpression was found to interact only weakly with the receptor and its signaling components (Fig. 3B). Exogenous NRAGE overexpression exceeded the level of naturally occurring NRAGE within a cell, but it highlighted the important binding capacities for NRAGE under changing cellular circumstances. We therefore assessed the binding interactions of endogenous NRAGE to the BMP signaling complex in the presence or absence of BMP-4. Endogenous NRAGE immunoprecipitated from NPCs was found to associate with BMPR-Ia and TAK1, TAB1, and XIAP only in the presence of BMP-4 (Fig. 3C). Therefore, from the observations that the association of endogenous NRAGE with the BMP receptor is ligand dependent and that reducing NRAGE levels within NPCs confers a significant attenuation to BMP-mediated apoptosis, we propose that NRAGE functions as a bona fide member of the BMP signaling pathway facilitating ligand-dependent apoptosis.

To demonstrate that NRAGE is required for activation of p38 by BMP-4, we observed p38 phosphorylation in cells that expressed NRAGE at normal and reduced levels. We also monitored p38 phosphorylation as a function of TAK1 levels. This latter experiment was a positive control, because TAK1 is a known upstream regulator of p38. As expected, reduction of TAK1 expression via antisense morpholinos drastically perturbed activation of p38 (Fig. 3D). More importantly, we found a similar reduction in p38 activation in cells in which TAK1 expression was normal but NRAGE levels were diminished, suggesting that, like TAK1, NRAGE is a key upstream regulator of p38 activity (Fig. 3D). The downregulation of NRAGE

expression appeared to have a specific effect on p38 activation because there was no change in the activation of Smad-1 or JNK as a result of BMP-4 treatment (Fig. 3D). These results demonstrate that the activation of noncanonical BMP signaling is accomplished through NRAGE's regulation of p38 activity.

NRAGE-mediated apoptosis requires canonical and noncanonical BMP pathways. Having established a connection between BMP signaling and NRAGE activation of p38 leading to cellular apoptosis, we performed a series of comparative experiments using both systems as they succumb to the apoptotic actions of RA and BMP-4 or NRAGE overexpression in order to delineate required BMPR signaling components. We have previously shown that diminishing NRAGE expression in both cell systems attenuates BMP apoptotic events. Moreover, the addition of SB203580 to inhibit p38 in NPCs when treated with RA and BMP-4 resulted in similar attenuation of apoptosis (Fig. 4A). The ability to rescue cell death was specific to p38 because concentrations up to 100 μM of the JNK inhibitor SP600125 failed to provide any significant gain in survival (data not shown), a finding which is consistent with the observation that JNK was not activated during apoptosis (Fig. 3D).

To further confirm a role for NRAGE in RA- and BMP-4-mediated apoptosis, we induced apoptosis in P19 cells by overexpressing NRAGE and tested the effect of treatment with the specific p38 inhibitor, SB203580. Annexin V labeling was used to detect cells in early phases of apoptosis (NRAGE-GFP$^+$/annexin V$^+$/7-AAD$^-$). After 48 h of overexpressing NRAGE, 57% ± 8% of the cells were annexin V immunoreactive, a significantly greater number than the 1% ± 2% in the control GFP-expressing cell population (Fig. 4Bd). NRAGE induced apoptosis was significantly attenuated through either reducing TAK1 protein or the addition of a dominant-negative Smad5 (TAK1 KD, 26% ± 4%; Smad5 DN, 24% ± 7%) (Fig. 4Bd). The latter result demonstrates that both aspects of BMP signaling appear to be prerequisites to signal downstream apoptotic events. In agreement with this, inhibition of p38 through SB203580 treatment in the NRAGE overexpressing cell population showed an impressive rate of survival 10% ± 9% (Fig. 4Be). Moreover, using the specific caspase-3 inhibitor, Z-DQMD-FMK, greatly enhanced cell survival (1% ± 1%) when NRAGE was overexpressed (Fig. 4Bf), suggesting that
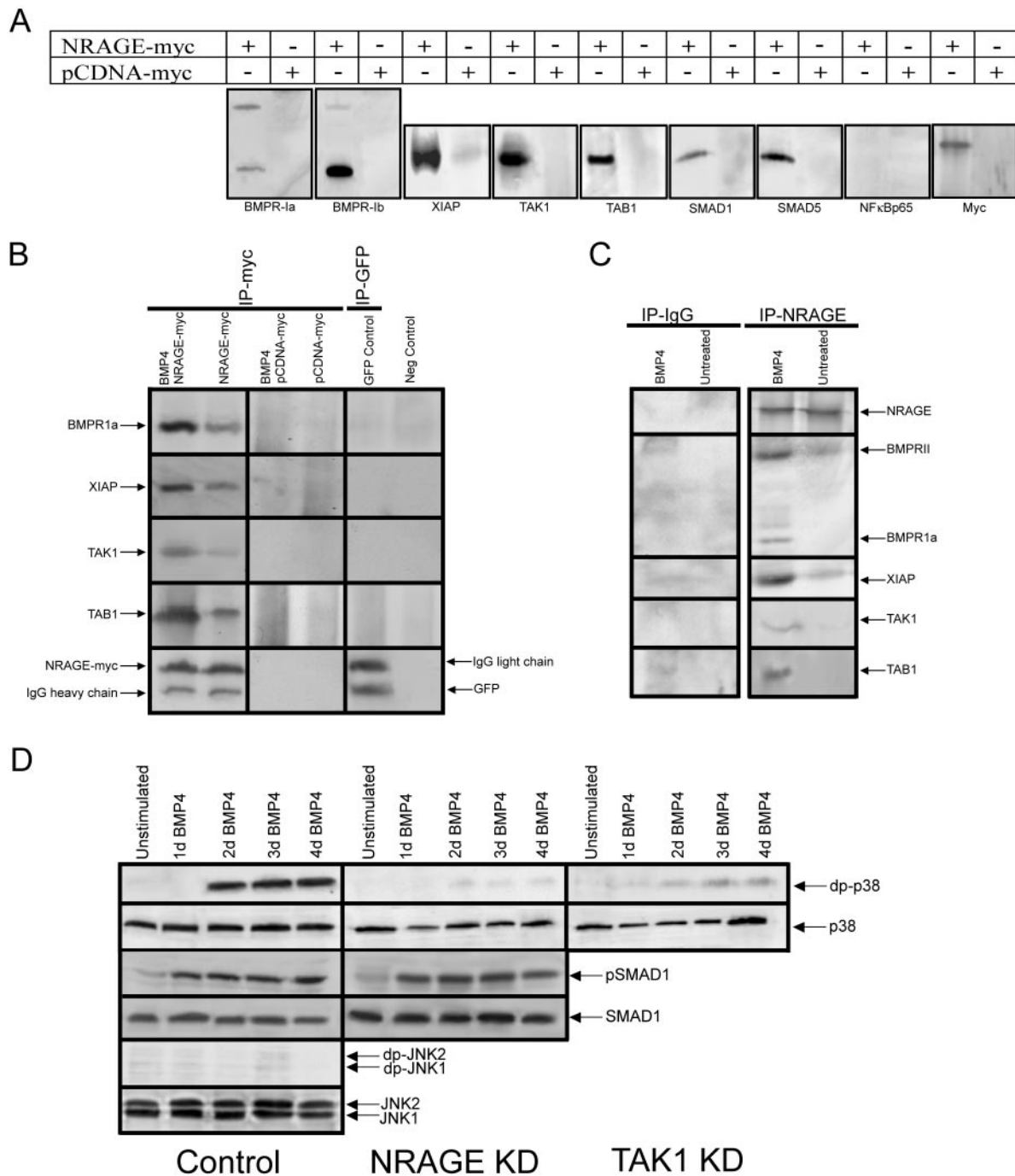
FIG. 3. NRAGE strongly interacts with members of the noncanonical BMP signaling pathway. (A) Western analysis was performed on lysates from P19 cells transiently overexpressing full-length NRAGE-myc treated with BMP-4 for 24 h. Immunoprecipitation of the resulting lysates for the myc tag were used to identify potential NRAGE-binding proteins. The resulting blots were probed for various members of the BMP signaling cascade. (B) NRAGE-myc was transiently overexpressed in P19 cells treated with or without BMP-4, and cell lysates were collected and immunoprecipitated. Note that BMP-4 treatment facilitated BMPR-Ia complex formation, whereas in the absence of ligand NRAGE interacted only minimally with receptor components. (C) Endogenous NRAGE was immunoprecipitated from NPCs after BMP-4 treatment. Only in the presence of BMP-4 did endogenous NRAGE interact with BMPR and its associated effectors. (D) Western blotting was used to detect active, doubly phosphorylated p38 in control cells, and cells were treated with either TAK or NRAGE morpholinos. Although all cells expressed similar levels of inactive p38, only control cells showed phosphorylation of p38. Reduced levels of NRAGE or TAK1 inhibited the appearance of active p38. In contrast, treatment with NRAGE morpholinos had no effect on the canonical BMP pathway, as indicated by the appearance of active Smad-1. JNK was not activated as a result of BMP-4 treatment.
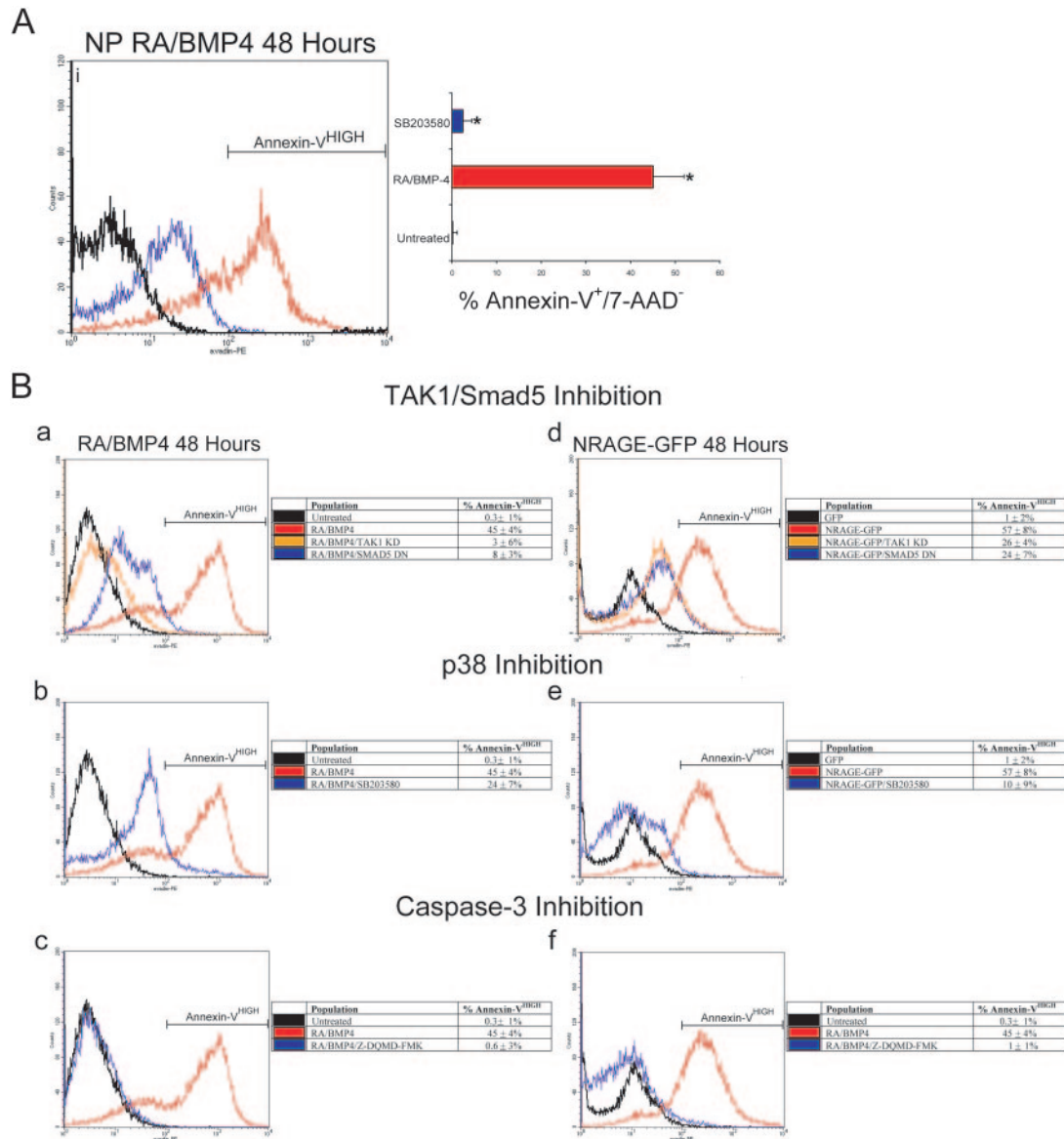
FIG. 4. Neural progenitors require p38 MAPK to mediate apoptosis. (A) Annexin V labeling was used to detect neural progenitor cells undergoing apoptosis in control, RA/BMP, or RA/BMP in the presence of the p38 inhibitor SB203580 (5 μM). The mean results ± the SD of four experiments demonstrate that inactivation of p38 rescues cells from apoptosis ($t = 7.2$; ∗, $P < 0.01$). (B) Representative FACS histograms of annexin V-stained cells in each condition with the means ± the SD of four separate experiments. RA, BMP-4, and NRAGE overexpression exhibited similar functional requirements to mediate apoptosis. (a to c) Reducing the expression of the canonical and noncanonical BMP signaling cascade components abrogated the ability of NRAGE to induce apoptosis in P19 cells. (d to f) When P19 cells expressing full-length NRAGE were deprived of canonical and noncanonical BMP signaling components, apoptosis was efficiently reduced.

the proapoptotic actions converge upon common apoptosis effector molecules.

As a final assurance for the involvement of NRAGE in BMP-mediated apoptosis, we treated P19 cells with RA and BMP-4 for a period of 48 h and subsequently determined the requirements for canonical and noncanonical BMP signaling. As was found with NRAGE overexpression, inhibition of either TAK1 or Smad5 signaling abolished the induction of apoptosis (TAK1 KD, 3% ± 6%; Smad5 DN, 8% ± 3%) (Fig. 4Ba). Furthermore, activation of p38 is also an important regulatory event, because inhibition of p38 by SB203580 was effective in reducing the level of cell death (24% ± 7%) (Fig.

4Bb), as was inhibiting caspase-3 (0.6% ± 3%) (Fig. 4Bc). Collectively, these studies demarcate NRAGE as a pivotal and necessary molecule in mediating the apoptotic effects of BMP in the developing central nervous system. However, even though NRAGE is specifically involved in the regulation of the noncanonical pathway, we have demonstrated that canonical signaling is indeed a necessary component. Therefore, the signal to undergo apoptosis mediated by BMP is hypothesized to be a collective sum of both aspects of the signaling cascades. It is not clear whether canonical and noncanonical signaling augment each other or whether opposing actions of these pathways lead to the initiation of cell death.
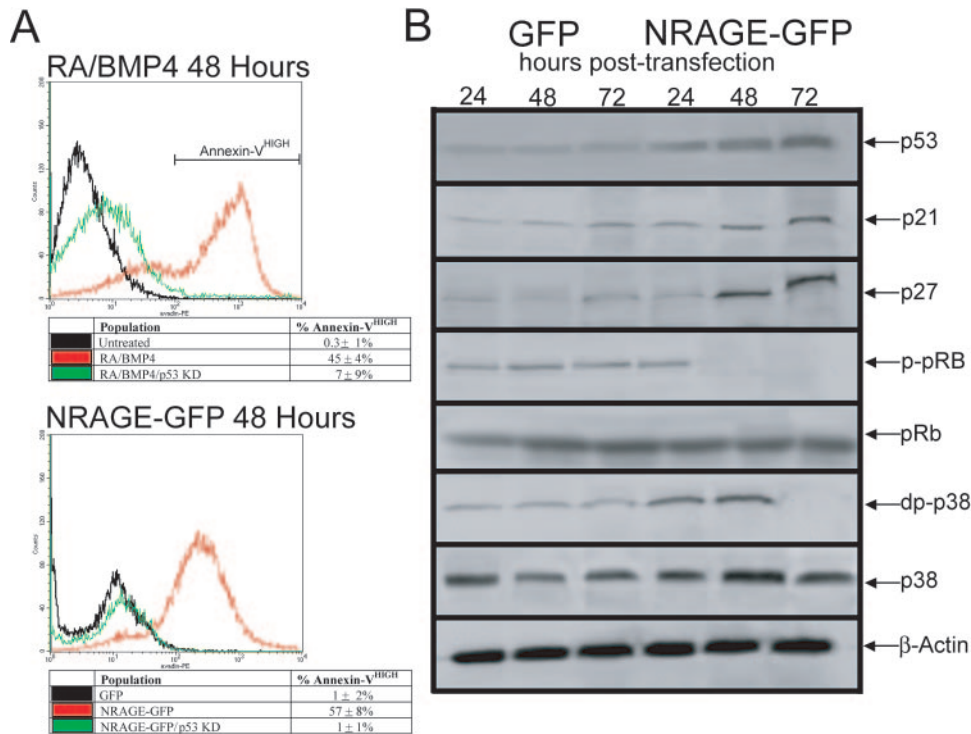
FIG. 5. NRAGE-mediated apoptosis is p53 dependent. (A) p53 knockdown or control morpholinos were introduced into P19 cells, which were treated with RA and BMP-4 or transiently transfected with NRAGE-GFP, and the percentage of apoptosis was determined by using annexin V binding. Both RA/BMP-4 and NRAGE-GFP induced apoptosis required p53 as a necessary component for cell death signaling. (B) NRAGE^{+GFP} cells were purified by using FACS 24, 48, and 72 h posttransfection. Cell lysates were collected and subjected to standard Western blotting techniques. As anticipated, NRAGE overexpression resulted in increased p53 levels. A direct consequence of increased p53 was the accumulation of p21^{waf1} and p27^{kip1} after prolonged exposure to NRAGE. This increase in CDK inhibitors was reflected in elevated levels of active p-pRb. Furthermore, in support of NRAGE as an activator of p38, overexpression significantly increased the active form of p38 within the first 48 h.

NRAGE regulates the G₁-S cell cycle transition. Recent data suggest that uncoordinated expression of cell cycle molecules and the consequent breach of cell cycle checkpoints could be one of the primary mechanisms by which neural progenitors undergo apoptotic death during terminal exit from the cell cycle. Evidence indicates that upregulation of cyclin/cyclin-dependent kinase activity at the G₁-to-S transition and deregulation of E2F transcription factors mark early stages of neuronal apoptosis (22). The observation that NRAGE-mediated apoptosis required both Smad and TAK1 signaling, which are both potent regulators of the cell cycle within NPCs, suggests that the induction of apoptosis is dependent on disruption of the cell cycle (6, 8, 33). Because of the intimate link between cell cycle and apoptosis, most often leading to induction of p53 when control is lost, we sought to address the contributions of p53 to both RA and BMP-4 and NRAGE-mediated apoptosis. P19 control and p53 knockdown cells were treated to undergo apoptosis using our standard RA and BMP-4 technique. After a 48-h treatment window, cells were collected and stained for annexin V and analyzed by using FACS. Abrogation of p53 was effective in preserving cell viability in RA- and BMP-4-treated cells (RA and BMP-4, 45% ± 4%; p53 KD, 7% ± 9%), likewise, NRAGE-mediated apoptosis was found to require p53 (NRAGE, 57% ± 8%; p53 KD, 1% ± 1%) (Fig. 5A). Li and coworkers found that NRAGE, when overexpressed, induced p53, which was indispensable for the induction of

p21^{waf1} leading to growth arrest (47). If NRAGE does facilitate apoptosis through a cell cycle-dependent mechanism, we would surmise that NRAGE-overexpressing cells should have elevated levels of p53 and CDKs.

To this end, cell lysates were collected from FACS-purified NRAGE^{+GFP} and control^{+GFP} cells at 24, 48, and 72 h post-transfection and subjected to standard Western analysis. As anticipated, p53 levels accumulated as time progressed, a finding supporting the hypothesis that NRAGE depended on p53-mediated apoptosis (Fig. 5A and B). In agreement with Li and coworkers, prolonged NRAGE expression resulted in elevated p21^{waf1} and p27^{kip1} levels, which was indicative of growth arrest. The activation of Rb by the 48-h mark further supports the notion that NRAGE overexpression facilitates mitotic arrest (Fig. 5B). These results are consistent with NRAGE^{+GFP}-induced G₁-S arrest after 72 h (38, 47). However, initiation of apoptosis in a cell cycle-dependent manner stimulated through BMP-NRAGE signaling implies that, if NRAGE is involved in the induction process, NRAGE must have functions in addition to being a growth arrest protein, such as the capacity to promote the required deregulation in the cell cycle need for the activation of the apoptotic pathway. We noted that NRAGE overexpression within the first 48 h significantly increased the level of active p38 (Fig. 5B), thus demonstrating that NRAGE is an activator of p38. Taken with the fact that NRAGE-p38 signaling is a necessary component for the in-
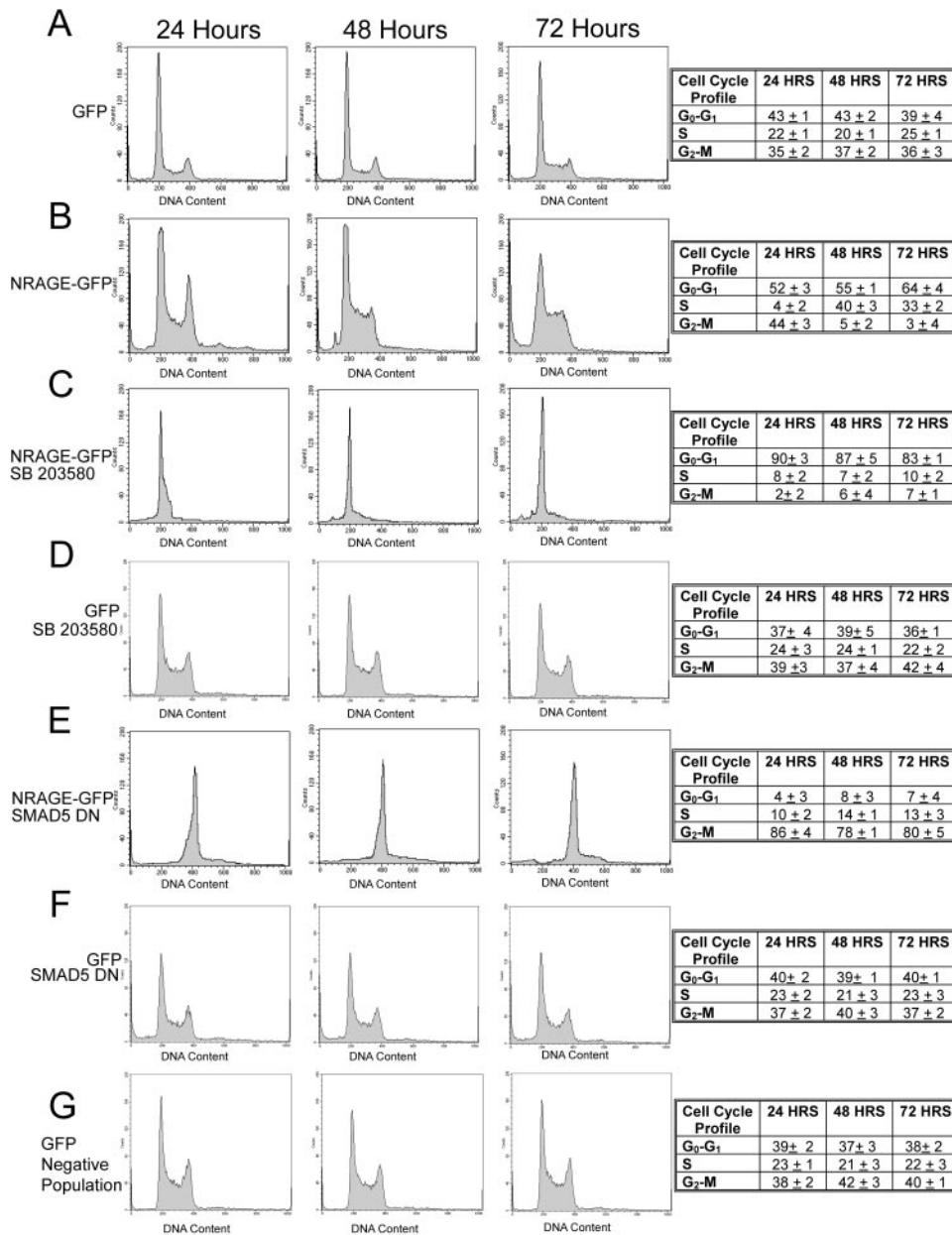
FIG. 6. NRAGE facilitates both growth arrest and progression through S phase. (A and B) NRAGE-GFP was overexpressed, cells were collected 24, 48, and 72 h posttransfection, and their cell cycle profile was analyzed by flow cytometry. After 24 h NRAGE was driving progression through the S phase with cells accumulating at the G_2-M transition. However, by 48 to 72 h NRAGE was facilitating a potent G_1-S arrest. (C and D). The ability of NRAGE to promote cell cycle progression required p38, since disruption of p38 signaling with SB203580 facilitated a rapid G_1 arrest. (E to G) Overexpression of both NRAGE and dominant-negative Smad5 resulted in cells accumulating in the G_2 phase.

duction of apoptosis, we sought to determine whether this aspect was responsible for progression through the cell cycle.

To dissect the specific contribution of NRAGE-TAK1-p38 and Smad-regulated effects on the cell cycle, cells overexpressing NRAGE-GFP (NRAGE^{+GFP}) were analyzed for DNA content by flow cytometry at 24, 48, and 72 posttransfection. After 24 h, NRAGE^{+GFP} cells exhibited an enhanced accumulation in G_2-M (44% ± 3%) relative to P19 cells transfected with GFP (control^{+GFP}) (35% ± 2%; t = 7.2, $P > 0.04$) (Fig. 6A and B). By 48 h, the majority (95% ± 4%) of NRAGE^{+GFP}

cells were positioned at the G_1-S transition compared to just 63% ± 3% (t = 9.6, $P > 0.02$) for control cells. The percentage of cells at G_1-S after 72 h was further enhanced (97% ± 6%) compared to GFP controls (64% ± 5%; t = 12.3, $P > 0.01$). This unique ability for NRAGE to initially provide cell cycle progression while later facilitating mitotic arrest reveals the important dichotomy that exists between TAK1 and Smad signaling. Therefore, we parsed individual contributions from each pathway to the cell cycle. We antagonized p38 signaling and observed a rapid and sustained G_1 arrest in NRAGE^{+GFP}

cells relative to control^{+GFP} cells (Fig. 6C and D). Moreover, the addition of a kinase-inactive dominant-negative mutant of TAK1 or TAK1-knockdown morpholino also yields a similar G$_1$ arrest (data not shown). These results suggest that NRAGE is responsible for cell cycle progression in a p38-dependent manner. Therefore, we hypothesized that in the absence of p38 signaling NRAGE would provide a rapid G$_1$ arrest. If the growth arrest observed in p38-antagonized NRAGE^{+GFP} cells is a consequence of elevated Smad signaling, then introduction of a dominant-negative Smad5 would inhibit growth arrest. Indeed, NRAGE^{+GFP} cells cotransfected with dominant-negative Smad5 displayed a striking G$_2$ arrest (Fig. 6E) compared to control^{+GFP}/dnSmad5$^+$ or NRAGE^{-GFP-}/dnSmad5$^-$ cells (Fig. 6F and G). These findings demonstrate the capability to disassociate specific aspects of NRAGE-mediated cell cycle control, revealing an antagonistic bipotential function of BMP signaling. This novel cell cycle control provides an attractive model whereby altering the level of Smad or TAK1 signaling a neural progenitor receives one effects a dynamic interplay between growth arrest and cell cycle progression.

NRAGE is required for cell cycle arrest and differentiation of multipotent progenitors. The coupled relationship between cell cycle and differentiation/apoptosis is modulated at multiple stages during development, in part through BMPs (3, 21, 23, 28). Recent evidence has suggested that appropriate levels of endogenous NRAGE are required to cooperate with Necdin to promote terminal differentiation of postmitotic myoblasts and neuroblasts by repressing cell proliferation (20). Likewise, antisense NRAGE morpholinos or control morpholinos were used to knockdown NRAGE protein expression in P19 cells. Cells were treated with RA to induce neurogenesis. The percentage of postmitotic neurons was calculated by using MAP2A/B expression; astrocytes were detected by GFAP expression, and proliferative multipoint neural progenitors were detected by using Nestin. Loss of NRAGE expression drastically perturbed the generation of neurons, and this deficit appeared to be the result of a failure of neural progenitors to withdraw from the cell cycle (Fig. 7A). The deficit was at the sole expense of neurogenesis, as was evident by an increase of 32% ± 5% in the number of multipotent progenitors with the ratio of glia remaining unaffected. Therefore, NRAGE appears to be a key component regulating the transition of multipotent progenitors to differentiated neuron.

To determine whether this inhibition in differentiation was a direct result of failure to induce appropriate gene expression, RNA was collected on days 1 through 4 of differentiation, and semiquantitative RT-PCR was performed. In RA-treated cultures NRAGE knockdown did not inhibit the induction of proneural gene expression (Fig. 7B). In fact, the loss of NRAGE accelerated RA-regulated gene expression by 24 h. Furthermore, using Oct3/4 as a general measure of the state of "stemness" and Hes1 as a determinant of the frequency of neural progenitors, NRAGE knockdown cells appeared to expand or maintain cells in a multipotent state. Therefore, the apparent incapacity to generate postmitotic neurons in NRAGE knockdown cells is not a deficit in early proneural gene expression per se but may reflect an imbalance between early proneural genes and antagonistic bHLH factors such as Hes1 and Hes5. Indeed, Hes1 expression was elevated to inappropriate levels as a result of loss of NRAGE, which may

directly contribute to the loss of late neurogenic genes such as MEF2A/C observed in NRAGE knockdown cells (Fig. 7B). Collectively, our results demonstration that BMP signaling through NRAGE is a potent regulator of the cell cycle required to mediate the differentiation of neural progenitors into postmitotic neurons but possesses the unique ability to facilitate apoptosis when deregulation of the differentiation pathway arises.

DISCUSSION

NRAGE plays a key role in the activation of p38 leading to apoptosis through BMP-4 treatment of neural progenitors. The presence of apoptosis in the proliferative neuroepithelium raises the question of how the balance between maintenance and depletion of the progenitor pool size is appropriately controlled by the extracellular environment (44). To elucidate the specific features of neural progenitor apoptosis during neocortical development, we took advantage of primary cortical NPCs and the P19 cell line. Both cell systems differentiate into neurons and glia when grown in the presence of RA. In addition to differentiation, RA also induces activation of caspase-9 and caspase-3 to promote apoptosis (5, 19, 30). Furthermore, the apoptotic action of RA is facilitated by the addition of BMP-2 or BMP-4 (9, 25).

In this study, we showed that NRAGE is a necessary and sufficient mediator of RA and BMP-4 induced apoptosis in both NPCs and P19 cells. NRAGE, which has been shown in the peripheral nervous system to mediate cell cycle withdrawal and NGF-p75^{NTR} cell apoptosis, was shown here to take part in BMP regulation of progenitor cell number in the forming cortex. The RA and BMP-4 apoptotic signal requires the activation of BMPR-Ia and subsequent formation of an NRAGE signaling complex involving TAK1, TAB1, and XIAP. Our results demonstrate the formation of the complex but do not reveal the nature of specific protein-protein interactions. However, Jordan et al. have previously shown that XIAP binds NRAGE through its RING domain (15). It is through this RING domain that XIAP also associates with BMPR-Ia (49). Therefore, it is conceivable that NRAGE's role in BMP signaling is a consequence of its binding to XIAP through the RING domain that is directly coupled to the BMP receptor. The interaction of NRAGE with members of the noncanonical BMP signaling cascade is required for the activation of p38, which subsequently leads to enhancing cell death. NRAGE plays a vital role in this pathway in that forced activation of NRAGE by overexpression leads to p38 and caspase activation, whereas eliminating or diminishing NRAGE expression rescues cell viability in the presence of BMP. These results suggest that NRAGE is a fulcrum between apoptosis and survival and that when associated with TAK1 and TAB1, NRAGE triggers death but is regulated by contact with XIAP. Therefore, unlike neurotrophin survival, in which cells are at the brink of death and compete for limited amounts of trophic support to quench the apoptotic signals, BMP-induced cell death is an instructive signal initiating a latent apoptotic pathway.

BMPs mediate cell death within neural progenitors. There appear to be two functionally distinct types of programmed cell death in the developing nervous system of mammals: an early
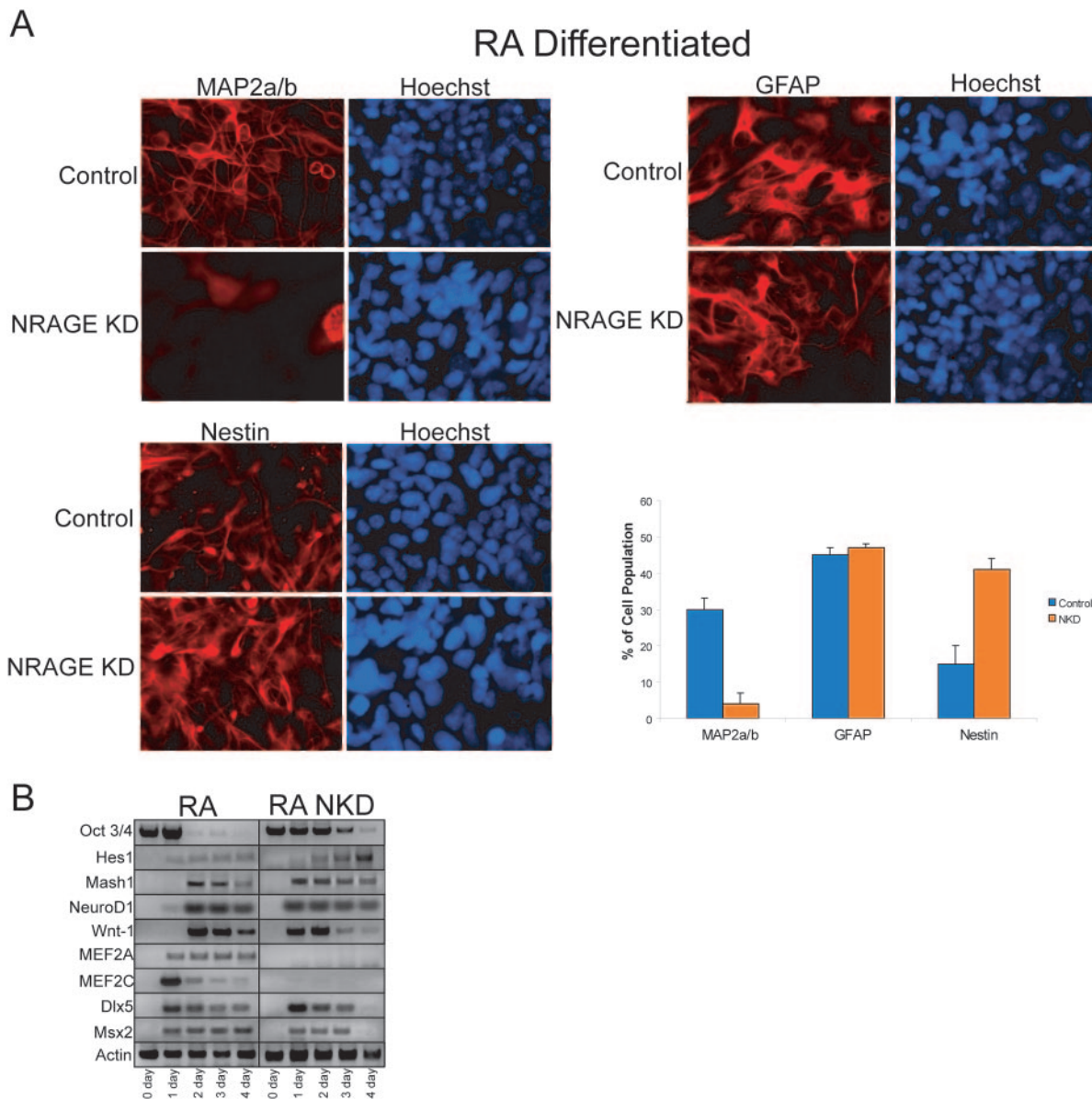
FIG. 7. NRAGE mediates the transition of multipotential neural progenitors to postmitotic neuron. (A) P19 embryonal carcinoma control or NRAGE knockdown cells were differentiated with RA for 4 days, cultured for an additional 4 days without RA, and then stained for the postmitotic neuron marker MAP2A/B, the glial marker GFAP, and Nestin for multipotential neural progenitors. In the absence of NRAGE, postmitotic neurons were not generated, and this deficit resulted in the accumulation of neural progenitors. Glial differentiation remained unaffected. To assess whether the inhibition was a result of perturbation in proneural gene expression, RT-PCR was performed on RA-stimulated control and NRAGE-knockdown cells were cultured as aggregates between 1 to 4 days. (B) Both Oct3/4 and Hes1 gene expression were elevated, suggesting NRAGE-knockdown cells remain as pluripotent neural progenitors. Loss of NRAGE accelerated the onset of early proneural gene expression and BMP-regulated genes. The expression of later proneural gene expression such as MEF2A and MEF2C was abolished.

cell death limiting the number of neural precursors and the more traditional mechanism of pruning unnecessary and misrouted postmitotic neurons based on trophic support (4). Reports have suggested that up to 70% of cortical neuroblasts in the proliferative ventricular zone undergo apoptosis, although the actual percentage must be <50% in order to expand the neural epithelium. Whatever the exact percentage, in murine species progenitor apoptosis commences at ~E10 and peaks at ~E13 before decreasing postnatally to the low levels in the adult (1, 2, 12, 46). This early programmed cell death coincides

well with both the spatial and temporal distribution of NRAGE (17). Given the evidence presented within, it seems logical that this early cell death is mediated through BMP-NRAGE signaling, resulting in the activation p38 leading to the initiation of the caspase cascade. This, along with the fact that NRAGE levels peak just prior to the onset of NPC apoptosis, further supports NRAGE as an important component mediating cell survival in the early cortex.

Our findings are in agreement with previous reports demonstrating a collaborative effort between TAK1- and TAB1-
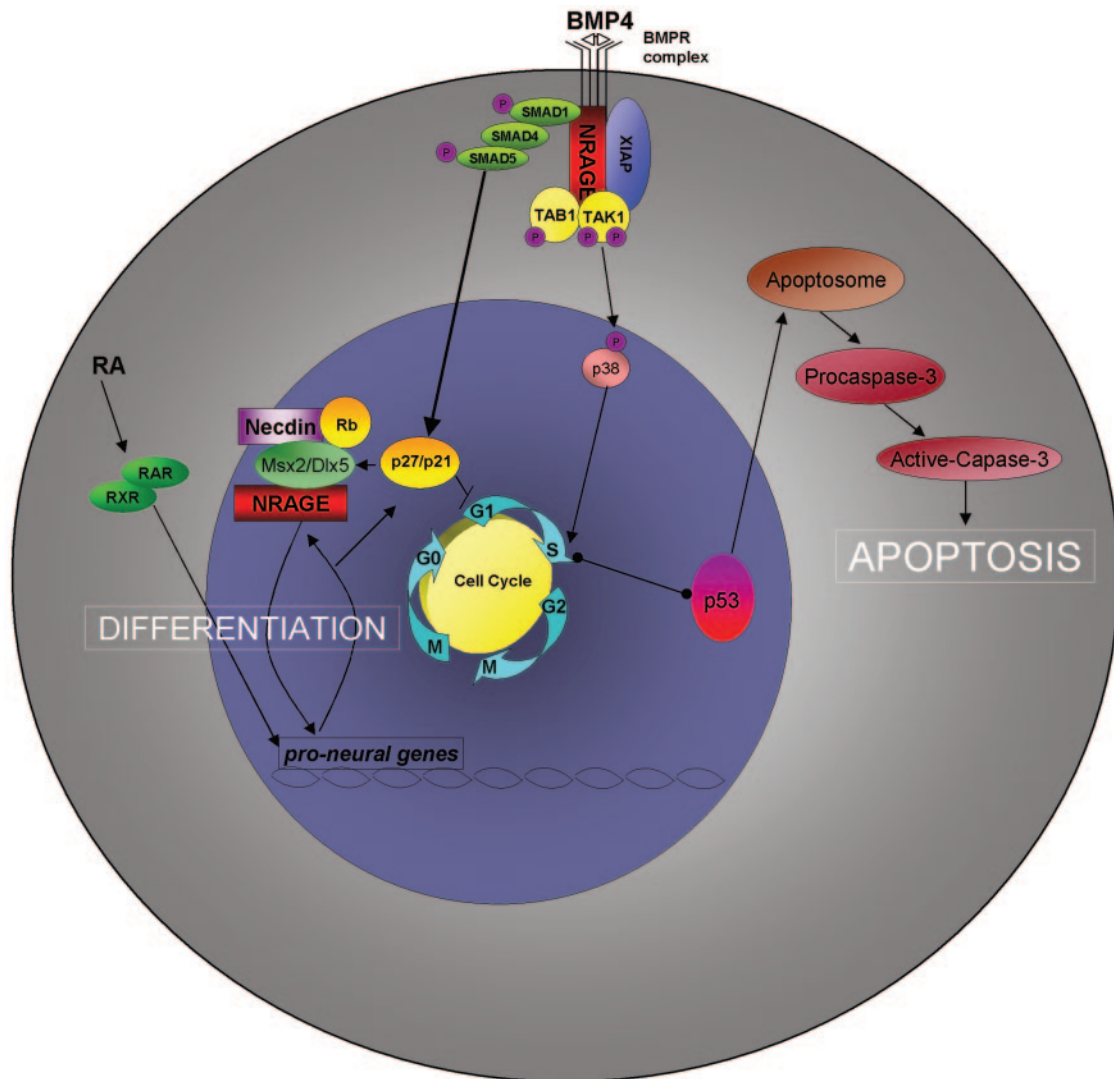
FIG. 8. Model of BMP-stimulated apoptosis through NRAGE signaling in neural progenitor cells. BMP stimulation triggers activation of NRAGE and its cooperation with the TAK1-TAB1-XIAP complex to activate p38. Active p38 promotes progression through the cell cycle, while Smad signaling facilitates growth arrest. This precocious reentry into S phase leads to the activation of p53 that facilitates activation and formation of the apoptosome, resulting in caspase activation. However, a basal level of NRAGE signaling is required to mediate growth arrest for terminal exit from the cell cycle in order to permit neural differentiation.

induced cell death in the ventralization the *Xenopus* embryo (40). The activation of TAK1 requires an association with TAB1 (37). Moreover, XIAP interaction with the cytoplasmic domain of BMPR-Ia enhanced the ventralization of TAB1-TAK1 but perturbed the apoptotic effect (49). There is increasing evidence that this proapoptotic effect is directly regulated by p38 and not by JNK activity that antagonizes the survival effects of FGF-MAPK signaling required for neural progenitor survival (10).

Neural progenitor apoptosis is an alternative fate to differentiation. Abrogation of NRAGE or TAK1 expression led to a decrease in p38 activation and reduced cell death. However, inhibition of Smad signaling also yielded a similar result. The question remains as to how parallel BMP signaling ultimately leads to cell death. An answer, in part, may lie in the observation that BMP signaling is critical for neural development in

the cortex (24, 27) and apoptosis (25, 33). Moreover, the induction of cortical apoptosis appears to be a failure to correctly exit the cell cycle and differentiate (22, 46). Timing is very important during neurogenesis and intrinsic and extrinsic events that modify the cell cycle program have drastic consequences, not only in effecting the proliferative capacity of young neural progenitors but in their survival as well. Indeed, the capacity for NRAGE to initially drive proliferation while enhancing growth arrest provided the proapoptotic signal. However, in the absence of NRAGE progenitors fail to exit the cell cycle, thereby significantly diminishing the number of post-mitotic neurons formed. These aspects of NRAGE during neurogenesis highlight the dynamic relationship between survival and apoptosis.

As such, we have generated a working model to incorporate NRAGE into the known functions of BMP signaling (Fig. 8).

BMP stimulation triggers activation of NRAGE and its cooperation with the TAK1-TAB1-XIAP complex to activate p38. Active p38 leads to an initial increase in cell proliferation. Moreover, NRAGE's association with Necdin and Smad targets such as Msx2 and Dlx5 ultimately provide the necessary drive to exit the cell cycle and fully differentiate (20). However, excessive signaling through both canonical and noncanonical pathways can provide conflicting information, leading to p53 accumulation and activation of the apoptosome. However, it is not known how differences between the signaling cascades are generated. Recently, BMPR-Ia, BMPR-Ib, and BMPR-II have been shown to exist as either a preformed hetero- or a homo-oligomeric complex on the cell surface (7). Moreover, the oligomerization mode of the receptors at the cell surface appears to determine the activation of downstream signaling. It has been proposed that when BMP binds the high-affinity receptor BMPR-Ia or BMPR-Ib and recruits BMPR-II into a hetero-oligomeric complex, p38 is preferentially activated. The other alternative is for BMP to bind simultaneously to the preformed hetero-oligomeric complex activating the Smad signaling pathway (32). Collectively, our results demonstrate the importance for how NRAGE functions in the BMP signaling cascade regulating the switch between differentiation and apoptosis of neural progenitors.

ACKNOWLEDGMENTS

REFERENCES

1. **Blaschke, A. J., K. Staley, and J. Chun.** 1996. Widespread programmed cell death in proliferative and postmitotic regions of the fetal cerebral cortex. Development **122:**1165–1174.
2. **Blaschke, A. J., J. A. Weiner, and J. Chun.** 1998. Programmed cell death is a universal feature of embryonic and postnatal neuroproliferative regions throughout the central nervous system. J. Comp. Neurol. **396:**39–50.
3. **Chang, M. Y., H. Son, Y. S. Lee, and S. H. Lee.** 2003. Neurons and astrocytes secrete factors that cause stem cells to differentiate into neurons and astrocytes, respectively. Mol. Cell Neurosci. **23:**414–426.
4. **de la Rosa, E. J., and F. de Pablo.** 2000. Cell death in early neural development: beyond the neurotrophic theory. Trends Neurosci. **23:**454–458.
5. **Fujita, E., A. Soyama, M. Kawabata, and T. Momoi.** 1999. BMP-4 and retinoic acid synergistically induce activation of caspase-9 and cause apoptosis of P19 embryonal carcinoma cells cultured as a monolayer. Cell Death Differ. **6:**1109–1116.
6. **Furuta, Y., D. W. Piston, and B. L. Hogan.** 1997. Bone morphogenetic proteins (BMPs) as regulators of dorsal forebrain development. Development **124:**2203–2212.
7. **Gilboa, L., A. Nohe, T. Geissendorfer, W. Sebald, Y. I. Henis, and P. Knaus.** 2000. Bone morphogenetic protein receptor complexes on the surface of live cells: a new oligomerization mode for serine/threonine kinase receptors. Mol. Biol. Cell **11:**1023–1035.
8. **Glozak, M. A., and M. B. Rogers.** 2001. Retinoic acid- and bone morphogenetic protein 4-induced apoptosis in P19 embryonal carcinoma cells requires p27. Exp. Cell Res. **268:**128–138.
9. **Glozak, M. A., and M. B. Rogers.** 1996. Specific induction of apoptosis in P19 embryonal carcinoma cells by retinoic acid and BMP2 or BMP4. Dev. Biol. **179:**458–470.
10. **Goswami, M., A. R. Uzgare, and A. K. Sater.** 2001. Regulation of MAP kinase by the BMP-4/TAK1 pathway in *Xenopus* ectoderm. Dev. Biol. **236:**259–270.
11. **Graham, A., P. Francis-West, P. Brickell, and A. Lumsden.** 1994. The signalling molecule BMP4 mediates apoptosis in the rhombencephalic neural crest. Nature **372:**684–686.
12. **Haydar, T. F., C. Y. Kuan, R. A. Flavell, and P. Rakic.** 1999. The role of cell death in regulating the size and shape of the mammalian forebrain. Cerebral Cortex **9:**621–626.
13. **Heldin, C. H., K. Miyazono, and P. ten Dijke.** 1997. TGF-β signalling from cell membrane to nucleus through SMAD proteins. Nature **390:**465–471.
14. **Ishitani, T., J. Ninomiya-Tsuji, S. Nagai, M. Nishita, M. Meneghini, N. Barker, M. Waterman, B. Bowerman, H. Clevers, H. Shibuya, and K. Matsumoto.** 1999. The TAK1-NLK-MAPK-related pathway antagonizes signalling between beta-catenin and transcription factor TCF. Nature **399:**798–802.
15. **Jordan, B. W., D. Dinev, V. LeMellay, J. Troppmair, R. Gotz, L. Wixler, M. Sendtner, S. Ludwig, and U. R. Rapp.** 2001. Neurotrophin receptor-interacting mage homologue is an inducible inhibitor of apoptosis protein-interacting protein that augments cell death. J. Biol. Chem. **276:**39985–39989.
16. **Kalyani, A. J., D. Piper, T. Mujtaba, M. T. Lucero, and M. S. Rao.** 1998. Spinal cord neuronal precursors generate multiple neuronal phenotypes in culture. J. Neurosci. **18:**7856–7868.
17. **Kendall, S. E., D. E. Goldhawk, C. Kubu, P. A. Barker, and J. M. Verdi.** 2002. Expression analysis of a novel p75^NTR signaling protein, which regulates cell cycle progression and apoptosis. Mech. Dev. **117:**187–200.
18. **Kimura, N., R. Matsuo, H. Shibuya, K. Nakashima, and T. Taga.** 2000. BMP2-induced apoptosis is mediated by activation of the TAK1-p38 kinase pathway that is negatively regulated by Smad6. J. Biol. Chem. **275:**17647–17652.
19. **Kobayashi, T., A. Shinozaki, T. Momoi, K. Arahata, and T. Tsukahara.** 1996. Identification of an interleukin-1β converting enzyme-like activity that increases upon treatment of P19 cells with retinoic acid as the proteasome. J. Biochem. **120:**699–704.
20. **Kuwajima, T., H. Taniura, I. Nishimura, and K. Yoshikawa.** 2004. Necdin interacts with the Msx2 homeodomain protein via MAGE-D1 to promote myogenic differentiation of C2C12 cells. J. Biol. Chem. **279:**40484–40493.
21. **Li, W., C. A. Cogswell, and J. J. LoTurco.** 1998. Neuronal differentiation of precursors in the neocortical ventricular zone is triggered by BMP. J. Neurosci. **18:**8853–8862.
22. **Liu, D. X., and L. A. Greene.** 2001. Neuronal apoptosis at the G_1/S cell cycle checkpoint. Cell Tissue Res. **305:**217–228.
23. **Mabie, P. C., M. F. Mehler, and J. A. Kessler.** 1999. Multiple roles of bone morphogenetic protein signaling in the regulation of cortical cell number and phenotype. J. Neurosci. **19:**7077–7088.
24. **Mabie, P. C., M. F. Mehler, R. Marmur, A. Papavasiliou, Q. Song, and J. A. Kessler.** 1997. Bone morphogenetic proteins induce astroglial differentiation of oligodendroglial-astroglial progenitor cells. J. Neurosci. **17:**4112–4120.
25. **Marazzi, G., Y. Wang, and D. Sassoon.** 1997. Msx2 is a transcriptional regulator in the BMP4-mediated programmed cell death pathway. Dev. Biol. **186:**127–138.
26. **Masuda, Y., A. Sasaki, H. Shibuya, N. Ueno, K. Ikeda, and K. Watanabe.** 2001. Dlxin-1, a novel protein that binds Dlx5 and regulates its transcriptional function. J. Biol. Chem. **276:**5331–5338.
27. **Mehler, M. F., P. C. Mabie, D. Zhang, and J. A. Kessler.** 1997. Bone morphogenetic proteins in the nervous system. Trends Neurosci. **20:**309–317.
28. **Mehler, M. F., P. C. Mabie, G. Zhu, S. Gokhan, and J. A. Kessler.** 2000. Developmental changes in progenitor cell responsiveness to bone morphogenetic proteins differentially modulate progressive CNS lineage fate. Dev. Neurosci. **22:**74–85.
29. **Moriguchi, T., N. Kuroyanagi, K. Yamaguchi, Y. Gotoh, K. Irie, T. Kano, K. Shirakabe, Y. Muro, H. Shibuya, K. Matsumoto, E. Nishida, and M. Hagiwara.** 1996. A novel kinase cascade mediated by mitogen-activated protein kinase kinase 6 and MKK3. J. Biol. Chem. **271:**13675–13679.
30. **Mukasa, T., Y. Khoroku, T. Tsukahara, M. Y. Momoi, I. Kimura, and T. Momoi.** 1997. Wortmannin enhances CPP32-like activity during neuronal differentiation of P19 embryonal carcinoma cells induced by retinoic acid. Biochem. Biophys. Res. Commun. **232:**192–197.
31. **Munoz-Sanjuan, I., and A. H. Brivanlou.** 2002. Neural induction, the default model and embryonic stem cells. Nat. Rev. Neurosci. **3:**271–280.
32. **Nohe, A., S. Hassel, M. Ehrlich, F. Neubauer, W. Sebald, Y. I. Henis, and P. Knaus.** 2002. The mode of bone morphogenetic protein (BMP) receptor oligomerization determines different BMP-2 signaling pathways. J. Biol. Chem. **277:**5330–5338.
33. **Panchision, D. M., J. M. Pickel, L. Studer, S. H. Lee, P. A. Turner, T. G. Hazel, and R. D. McKay.** 2001. Sequential actions of BMP receptors control neural precursor cell production and fate. Genes Dev. **15:**2094–2110.
34. **Price, D. J., S. Aslam, L. Tasker, and K. Gillies.** 1997. Fates of the earliest generated cells in the developing murine neocortex. J. Comp. Neurol. **377:**414–422.
35. **Qian, X., A. A. Davis, S. K. Goderie, and S. Temple.** 1997. FGF2 concentration regulates the generation of neurons and glia from multipotent cortical stem cells. Neuron **18:**81–93.
36. **Qian, X., Q. Shen, S. K. Goderie, W. He, A. Capela, A. A. Davis, and S. Temple.** 2000. Timing of CNS cell generation: a programmed sequence of neuron and glial cell production from isolated murine cortical stem cells. Neuron **28:**69–80.
37. **Sakurai, H., H. Miyoshi, J. Mizukami, and T. Sugita.** 2000. Phosphorylation-dependent activation of TAK1 mitogen-activated protein kinase kinase kinase by TAB1. FEBS Lett. **474:**141–145.
38. **Salehi, A. H., P. P. Roux, C. J. Kubu, C. Zeindler, A. Bhakar, L. L. Tannis,

J. M. Verdi, and P. A. Barker. 2000. NRAGE, a novel MAGE protein, interacts with the p75 neurotrophin receptor and facilitates nerve growth factor-dependent apoptosis. Neuron **27:**279–288.

39. **Sasaki, A., Y. Masuda, K. Iwai, K. Ikeda, and K. Watanabe.** 2002. A RING finger protein Praja1 regulates Dlx5-dependent transcription through its ubiquitin ligase activity for the Dlx/Msx-interacting MAGE/Necdin family protein, Dlxin-1. J. Biol. Chem. **277:**22541–22546.

40. **Shibuya, H., H. Iwata, N. Masuyama, Y. Gotoh, K. Yamaguchi, K. Irie, K. Matsumoto, E. Nishida, and N. Ueno.** 1998. Role of TAK1 and TAB1 in BMP signaling in early *Xenopus* development. EMBO J. **17:**1019–1028.

41. **Shibuya, H., K. Yamaguchi, K. Shirakabe, A. Tonegawa, Y. Gotoh, N. Ueno, K. Irie, E. Nishida, and K. Matsumoto.** 1996. TAB1: an activator of the TAK1 MAPKKK in TGF-β signal transduction. Science **272:**1179–1182.

42. **Shirakabe, K., K. Yamaguchi, H. Shibuya, K. Irie, S. Matsuda, T. Moriguchi, Y. Gotoh, K. Matsumoto, and E. Nishida.** 1997. TAK1 mediates the ceramide signaling to stress-activated protein kinase/c-Jun N-terminal kinase. J. Biol. Chem. **272:**8141–8144.

43. **Smith, A., and A. Graham.** 2001. Restricting Bmp-4 mediated apoptosis in hindbrain neural crest. Dev. Dyn. **220:**276–283.

44. **Sommer, L., and M. Rao.** 2002. Neural stem cells and regulation of cell number. Prog. Neurobiol. **66:**1–18.

45. **ten Dijke, P., K. Miyazono, and C. H. Heldin.** 1996. Signaling via hetero-oligomeric complexes of type I and type II serine/threonine kinase receptors. Curr. Opin. Cell Biol. **8:**139–145.

46. **Thomaidou, D., M. C. Mione, J. F. Cavanagh, and J. G. Parnavelas.** 1997.

47. Apoptosis and its relation to the cell cycle in the developing cerebral cortex. J. Neurosci. **17:**1075–1085.

47. **Wen, C. J., B. Xue, W. X. Qin, M. Yu, M. Y. Zhang, D. H. Zhao, X. Gao, J. R. Gu, and C. J. Li.** 2004. hNRAGE, a human neurotrophin receptor interacting MAGE homologue, regulates p53 transcriptional activity and inhibits cell proliferation. FEBS Lett. **564:**171–176.

48. **Williams, M. E., P. Strickland, K. Watanabe, and L. Hinck.** 2003. UNC5H1 induces apoptosis via its juxtamembrane region through an interaction with NRAGE. J. Biol. Chem. **278:**17483–17490.

49. **Yamaguchi, K., S. Nagai, J. Ninomiya-Tsuji, M. Nishita, K. Tamai, K. Irie, N. Ueno, E. Nishida, H. Shibuya, and K. Matsumoto.** 1999. XIAP, a cellular member of the inhibitor of apoptosis protein family, links the receptors to TAB1-TAK1 in the BMP signaling pathway. EMBO J. **18:**179–187.

50. **Yamaguchi, K., K. Shirakabe, H. Shibuya, K. Irie, I. Oishi, N. Ueno, T. Taniguchi, E. Nishida, and K. Matsumoto.** 1995. Identification of a member of the MAPKKK family as a potential mediator of TGF-β signal transduction. Science **270:**2008–2011.

51. **Yao, Z., G. Zhou, X. S. Wang, A. Brown, K. Diener, H. Gan, and T. H. Tan.** 1999. A novel human STE20-related protein kinase, HGK, that specifically activates the c-Jun N-terminal kinase signaling pathway. J. Biol. Chem. **274:**2118–2125.

52. **Zhang, D., M. F. Mehler, Q. Song, and J. A. Kessler.** 1998. Development of bone morphogenetic protein receptors in the nervous system and possible roles in regulating trkC expression. J. Neurosci. **18:**3314–3326.